Journal of Theoretical and Applied Vibration and Acoustics 11 (1) 40-56 (2025)

I S A V

Journal of Theoretical and Applied Vibration and Acoustics

journal homepage: http://tava.isav.ir

Nonlinear analysis and numerical study of vortex bladeless turbine with experimental verification

Seyed Saeid Mansouri, Mohammad Reza Elhami *, Pouya Sarvi

Mechanical Engineering Department, Imam Hossein University, Tehran, IRAN

Research Article

ARTICLE INFO

Article history:
Received 17 September 2024

Received in revised form
8 January 2025

Accepted 22 February 2025

Available online 2 May 2025

Keywords:
Bladeless turbine

Parameter sensitivity analysis

Nonlinear

Harmonic balance method

ABSTRACT

With the growth of societies and the complexity of industry and technology, the human need for energy sources and the use of renewable energies, such as wind and sun, have been increasing. One way to achieve clean and renewable energies is the development of wind turbines. In this article, the development and parameter sensitivity analysis of a vortex bladeless turbine have been discussed. This type of turbine is made of a mast (fiberglass) connected to the ground by a rod (made of fiberglass). When the mast is exposed to an airflow, the pressure change causes von Karman vortices, and as a result, the mast starts to vibrate in the direction perpendicular to the fluid flow. Finally, electricity can be harvested by electromagnetic or piezoelectric mechanisms due to the displacement created. This article aims to maximize energy harvesting, which will occur in the highest range of displacement. By doing so, the nonlinear equations governing this problem are derived, and the effective parameters in the displacement (diameter of the mast and base, height of the mast and base, and density) with the objective function of the highest displacement have been analyzed. The vortex bladeless turbine was simulated as a fluid-structure interaction in ANSYS software, and the results were evaluated using an analytical solution. Finally, the experimental prototype was prepared, and the displacement of the mast was investigated and evaluated with analytical results.

* Corresponding author.
E-mail address: mrelhami.63@gmail.com (M.R. Elhami)

http://dx.doi.org/10.22064/tava.2025.2041373.1247

1. Introduction

Vortex bladeless turbine uses the vibrations caused by von Karman vortices to harvest energy [1]. Therefore, the dynamic investigation of this type of turbine and improving the vibration performance with the changes in the influencing parameters are crucial. One of the vital factors is the location of the turbine installation, which will determine the velocity of the upstream flow [2]. In this article, the speed is considered to be about 6.8 m/s. Another important factor is the amount of energy required, which determines the dimensions of the turbine. A bladeless turbine with a height of 13 meters is expected to produce about 4 kW of electricity (needed for a residential unit) [3]. According to the experimental limitations, the height of the turbine is considered to be 1.5 meters in this study. The connection of the flexible base to the mast is considered to be at the geometric center of the mast, which transmits the highest force to vibrate the system [4]. Here, the effective parameters, such as the diameter of the mast, the diameter of the flexible rod, the height of the mast, the height of the base, etc., have been investigated to maximize the displacement. As a result, the amount of energy harvesting will increase. Then, the dynamic behavior of the vortex bladeless turbine was evaluated analytically and numerically in variable conditions, and finally, an experimental prototype was built and tested. In 2017, Chizfahm et al. [5] investigated the analytical model for the movement of bladeless turbines with different cross-sections; they used the Euler-Bernoulli beam theory to simulate the dynamic and vibrational behavior of the bladeless turbine and used the Galerkin method to reduce the degree of the nonlinear equations. In 2020, Cajasa et al. [6] numerically investigated a vortex bladeless turbine and used Flex software. Parameters such as the highest displacement of the top of the mast in different conditions and the Reynolds number were investigated. Isam Bahadur [7] published an article entitled "Analysis of the dynamic model of vortex bladeless turbine" in 2022. The coupled nonlinear equations are developed according to the physics of the problem, with the concentrated mass model and the Lagrange equation.

In 2021, Raghunashi [8] investigated different materials for a vortex bladeless turbine and numerically checked the outputs at different frequencies. The research suggested using fiberglass polymer for the mast and carbon fiber polymer for the oscillating base, which is also used in this article. Singsten et al. [9] conducted a numerical study of a vortex bladeless turbine in the form of a circular cylinder clamped to the ground in 2019. This article used the RANS-SST model to simulate the flow at the Reynolds number of 105. This research placed two turbines back to back at a certain distance. Their findings show that due to the disturbance created in the downstream flow of the first turbine, the displacement in the second turbine is larger, resulting in higher energy harvest. In 2023, Jauvtis et al. [10] investigated the bladeless turbine at the Reynolds number of 300. They numerically analyzed the design parameter of the ratio of the height to the diameter of the mast in the ANSYS software. This research used the K-ε model to simulate the turbulent flow, which has a relatively low solution accuracy. Finally, this article obtained the maximum diameter-to-length ratio of 1 to 10. In 2021, Bagheri et al. [11] conducted a research under the title of energy harvesting from the phenomenon of nonlinear vibrations of bladeless turbines to further investigate this type of turbine. The selected model shows a single-ended beam that generates electricity using piezoelectricity. In this research, by extracting equations and solving them in MATLAB software, the structure was investigated in nonlinear mode. According to the studies, the following will be examined as a supplement to the previous studies on this issue: the vortex bladeless turbine parameter sensitivity analysis considering nonlinear equations and measuring effective parameters, 3D numerical solution of bladeless turbines in the state of FSI coupling, producing a

prototype with real dimensions and checking the displacement range of the turbine at different speeds and validating the analytical results with the experimental prototype.

2. Modeling and sensitivity analysis of design parameters

The vortex bladeless turbine consists of a flexible base attached to the rigid body of the mast [12]. The flexible base provides the conditions for the vibrations of the wind turbine system, while the mast is responsible for generating aerodynamic oscillating force by the flow, based on the effect of von Karman vortices [13]. The schematic of the turbine configuration is shown in Figure 1. The aerodynamic force applied to the turbine base is ignored due to the small diameter of the base and the much lower force than the force produced by the mast.

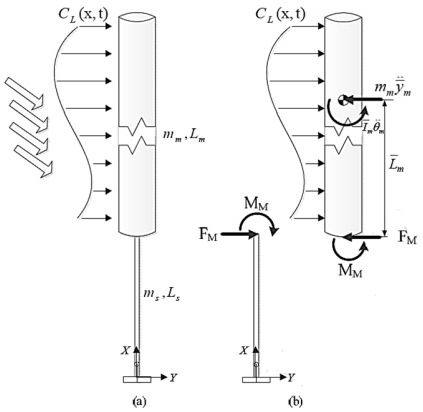

Fig. 1: Considering the bladeless turbine as an Euler-Bernoulli beam [5]

As shown in Figure 1, a force and a moment on the tip of the flexible base replace the total force from the pressure distribution caused by the fluid flow on the rigid mast; this process makes it possible to use Euler Bernoulli's cantilever beam theory for the vibration analysis of this system. Using the single-mode Galerkin method, the kinetic energy and the potential energy of the system are obtained as follows [14]:

$$T = \frac{1}{2}\int_0^{L_s} \dot{Y}^2(x,t)m\,dx = \frac{1}{2}\sum_i\sum_j \dot{y}_i(t)\dot{y}_j(t)\int_0^{L_s} \emptyset_i(x)\emptyset_j(x)m\,dx = \frac{1}{2}\sum M_i\dot{y}_i^2(t) \quad (1)$$

$$U = \frac{1}{2}\int_0^{L_s} EIY''^2(x,t)\,dx = \frac{1}{2}\sum_i\sum_j y_i(t)y_j(t)\int_0^{L_s} EI\emptyset''_i(x)\emptyset''_j(x)\,dx = \frac{1}{2}\sum K_i y_i^2(t) \quad (۲)$$

In Equations (1) and (2), T is kinetic energy, U is potential energy, M_i is the generalized mass, K_i is the generalized stiffness, Y(x,t) is the transverse displacement of the turbine and $\emptyset$, and y are called the mode shape and the modal response factor. The work done by the oscillating force of the distributed lift and the mass and inertia of the wind turbine mast are calculated according to Equation (3):

$$\delta W = F_M\delta Y(L_s,t) + M_M\delta\theta(L_s,t) = F_M(\sum \emptyset_i(L_s)\delta y_i(t)) + M_M(\sum \emptyset'_i(L_s)\delta y_i(t)), \quad (۳)$$

where F_M and M_M are the force and moment produced by the wind turbine mast on the tip of the turbine base. By placing the equations in the Lagrange equation, the nonlinear equations are extracted as follows [5]:

$$M\ddot{y}(t) + \left[\frac{2\alpha}{D\omega_s}\right]\Gamma\dot{y}(t) + Ky(t) = \Gamma q(t) \tag{٤}$$

$$\left(\ddot{q}(t) - \omega_s G C_{L0}^2 \dot{q}(t) + {\omega_s}^2 q(t)\right) + \left(4\omega_s G q^2(t)\dot{q}(t)\right)\frac{\int_{L_s}^{L_s+L_m} h(x)^3\,dx}{\int_{L_s}^{L_s+L_m} h(x)\,dx} = \left[\omega_s F\frac{\dot{y}(t)}{D}\right] \tag{٥}$$

where $q(t)$ is the excitation component of the fluctuating lift coefficient, ω_s denotes vortex shedding frequency, C_{L0}, G, F are empirical parameters, and M, K, Γ, and h(x) are defined as follows [5] :

$$M = \int_0^{L_s} \emptyset^2(x) m_s\,dx + m_m\left[\emptyset^2(L_s) + \left(\overline{L}_m + \frac{L_m}{2}\right)\phi\phi'(L_s) + \left(\frac{\overline{L}_m L_m}{2} + \frac{\overline{I}_m}{m_m}\right)\emptyset'^2(L_s)\right] \tag{٦}$$

$$K = \int_0^{L_s} EI(\emptyset"(x))^2\,dx \tag{٧}$$

$$\Gamma = \frac{1}{2}\rho V^2 D\int_{L_s}^{L_s+L_m}[\,\phi^2(L_s) + (x-L_s)(2\phi(L_s)\phi'(L_s) + 2(x-L_s)\phi'^2(L_s))]\,dx \tag{8}$$

$$h(x) = \phi(L_s) + (x-L_s)\phi'^{(L_s)} \tag{9}$$

The nonlinearity in Vortex-Induced Vibrations (VIV) arises from several physical sources related to the interactions between the fluid flow and the structural dynamics. These nonlinearities are intrinsic to the complex nature of fluid-structure interactions and are caused by the following factors:

- The fluid forces driving VIV are inherently nonlinear because of the nature of vortex shedding and flow separation around the structure. These forces depend on several factors.
- The vortex shedding process generates oscillatory lift and drag forces that are not linearly proportional to flow speed or structural motion.
- The fluid forces depend on the amplitude of the oscillations, especially at large amplitudes, altering the vortex shedding pattern and changing the forces acting on the structure.
- The relationship between fluid velocity, viscosity, and vortex shedding frequency leads to nonlinear behavior across different flow regimes.

It is assumed that there is a phase difference in a certain excitation to solve the nonlinear equation governing the Couple system [15]. Therefore, the vibration of a vortex bladeless turbine is governed by Equation (10) and (11):

$$M\ddot{y}(t) + \left[\frac{2\alpha}{D\omega_s}\right]\Gamma\dot{y}(t) + Ky(t) - \Gamma q(t) = a_1 cos\omega t - a_2 sin\omega t \tag{10}$$

$$\left(\ddot{q}(t) - \omega_s G C_{L0}^2 \dot{q}(t) + {\omega_s}^2 q(t)\right) + \left(4\omega_s G q^2(t)\dot{q}(t)\right)\frac{\int_{L_s}^{L_s+L_m} h(x)^3\,dx}{\int_{L_s}^{L_s+L_m} h(x)\,dx} - \left[\omega_s F \frac{\dot{y}(t)}{D}\right] = a_3 cos\omega t - a_4 sin\omega t \tag{11}$$

Coefficients a_1 to a_4 are equivalent excitation amplitudes and are assumed as follows:

$$({a_1}^2 + {a_2}^2)^{\frac{1}{2}} = 0 \tag{12}$$

$$({a_3}^2 + {a_4}^2)^{\frac{1}{2}} = 0 \tag{13}$$

The assumptions made for the analytical solution of Equations (10) and (11) are the methods used to calculate the response of nonlinear equations using the harmonic balance method [16]. They are mostly used for nonlinear systems due to geometric parameters and inertia. The harmonic balance method describes Kirchhoff's law in the frequency domain and starts with a selected number of harmonics. This method assumes that the solutions can be represented by a linear combination of sine functions [17]. Therefore, as a first approximation, the answers are considered as follows:

$$q_1 = q_0 cos\omega t, \tag{14}$$

$$y_1 = y_0 cos\omega t, \tag{15}$$

which will be obtained by substituting the equations:

$$(-M\omega^2 y_0 + K y_0 - \Gamma q_0)^2 - \left(\left[\frac{2\alpha}{D\omega_s}\right]\Gamma\omega y_0\right)^2 = 0 \tag{16}$$

$$((-\omega^2 + {\omega_s}^2)q_0)^2 + \left(\omega_s G C_{L0}^2 \omega q_0 + \frac{\omega_s}{D} F\omega y_0 - (\omega_s G \omega {q_0}^3)\frac{\int_{L_s}^{L_s+L_m} h(x)^3\,dx}{\int_{L_s}^{L_s+L_m} h(x)\,dx}\right)^2 = 0 \tag{17}$$

Equations (16) and (17) are the analytical response of the nonlinear system, obtained using the harmonic balance method. Using the equations obtained, one may verify and evaluate the results with the results obtained by Chizfahm [5]. The following presents the validation of the analytical results obtained with the reference [5] and the investigation and analysis of the nonlinear phenomena in the relations. The wind turbine system is first studied based on the physics presented in the article [5] to verify the results.

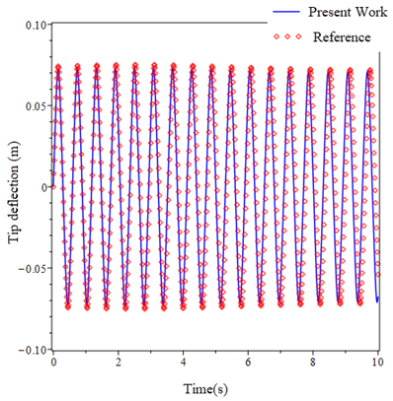

Fig. 2: Verification of system time response results with reference results [5] at a speed of 3.6 m/s

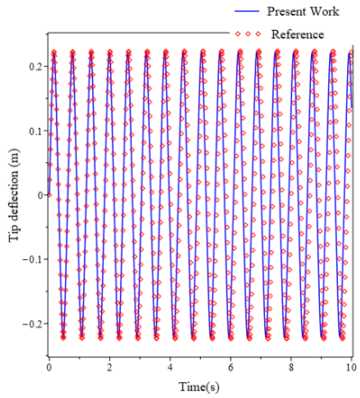

Fig. 3: Verification of system time response results with reference results [5] at a speed of 4.9 m/s

The results obtained from the present analytical solution have been compared with the numerical results of reference [5] at a speed of 3.6 m/s and 4.9 m/s, as shown in Figures 2 and 3, respectively. As it is clear, the two graphs are accurate. Thus, the obtained equations are used for parameter sensitivity analysis in the next part.

2.1. Nonlinear analysis of design parameters

This section investigates the main design parameters using the harmonic balance analytical method to increase the turbine's displacement amplitude [17]. To investigate the effects of flow speed, the dimensionless frequency Ω is used, which is defined as ($\boldsymbol{\Omega} = \frac{\boldsymbol{\omega_s}}{\boldsymbol{\omega_n}}$). The results indicate that the principle of superposition of forces does not hold in the governing equations, meaning the problem cannot be accurately predicted using linear relations. Frequency response curves are used to discuss local optimization. Unlike the time response, the frequency response shows the nonlinear effects on the system well.

Table 1: Assumptions of local optimization of vortex bladeless turbine

Mast Young's modulus (E) (GPa)	61.5
Rod Young's modulus (E) (GPa)	248.3
Mast length (cm)	70-150
Rod length(cm)	60-110
Mast diameter(mm)	80-140
Rod diameter(mm)	6-26
Mast thickness (mm)	2.5

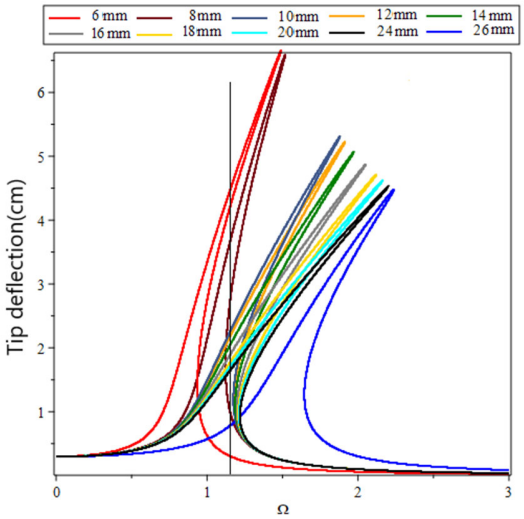

Fig. 4: Study of the effects of the base diameter on the frequency response of the turbine

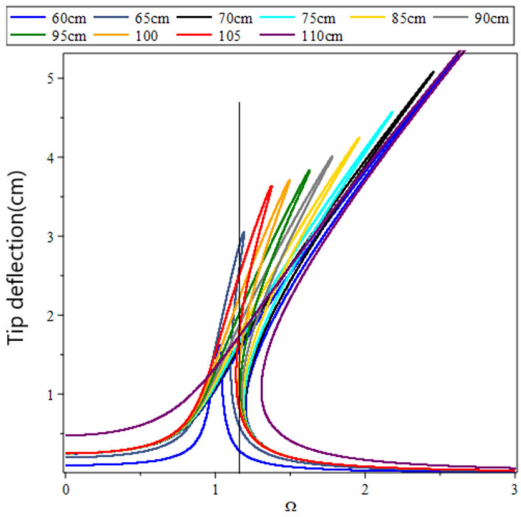

Fig. 5: Study of the effects of the base length on the frequency response of the turbine

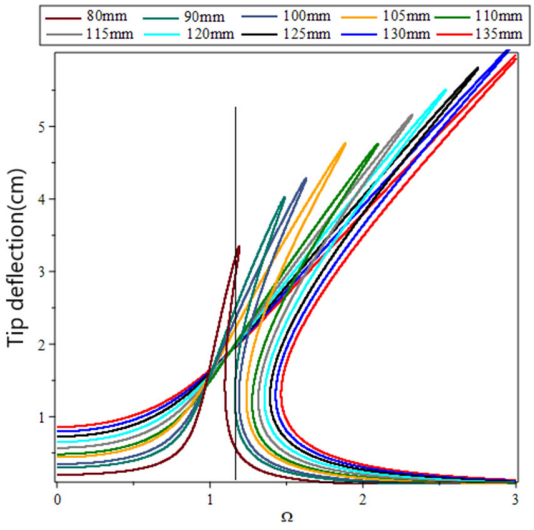

Fig. 6: Study of the effects of the Mast diameter on the frequency response of the turbine

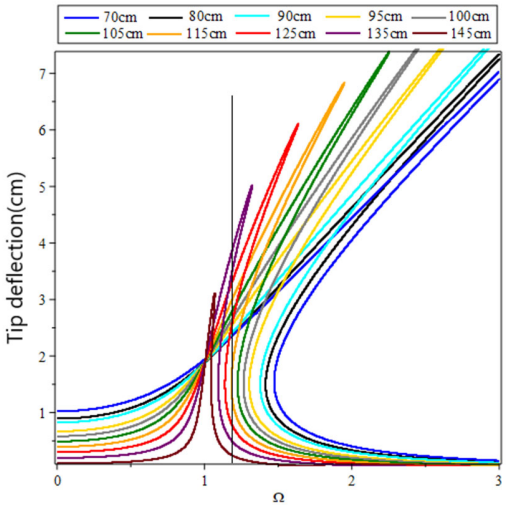

Fig. 7: Study of the effects of the Mast length on the frequency response of the turbine

- According to the shape of the frequency response shown in Figure 4, ten base diameters have been investigated. Considering that the excitation current frequency is in the range of 1.15, the blue curve corresponding to the base diameter of 10 mm will have the greatest response.
- The effects of turbine base length on system response have been studied, and the results are shown in Figure 5. The length of the turbine base has been investigated in ten modes. The base length is effective on many parameters, including the nonlinear behavior of the response. The base length of 100 cm will have the greatest response.

- By changing the physics of the problem, the natural frequency of the system changes. Thus, the maximum displacement can occur at different flow rates. According to the frequency response shown in Figure 6, the diameter below 10 cm will have more displacement at the flow speed of 6.8 m/s.
- The effects of the mast height on the frequency response of the turbine have been studied in the frequency response curve, and the results are shown in Figure 7. The designer would choose the blue curve showing the system's response at a mast height of 100 cm, as this response is within the flow velocity range of 6.8 m/s.

The time response of the tip of the mast, as well as the lift force, are shown at three velocities of 5.7, 6.8, and 7.9 m/s in Figures (8) to (10), respectively. As it is clear, increasing the flow velocity increases the amount of displacement, ultimately increasing the turbine's efficiency. The maximum displacement occurs at the excitation frequency, close to the lock-in region.

According to the results obtained in this section and the investigations carried out, in the ratio of frequencies higher than one, it is better to do the parameter sensitivity analysis nonlinearly and solve the equations by considering the non-linearizing factor of the system.

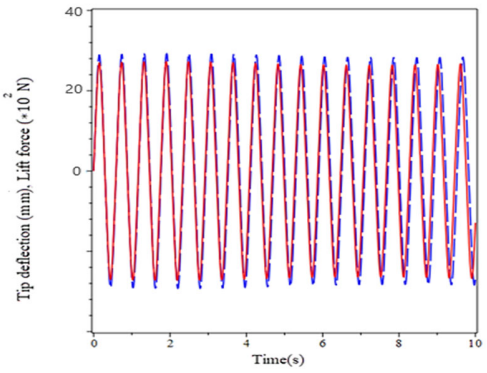

Fig. 8: Response of turbine end (blue broken line) and lift force (red continuous line) due to wind flow with a speed of 5.7 m/s

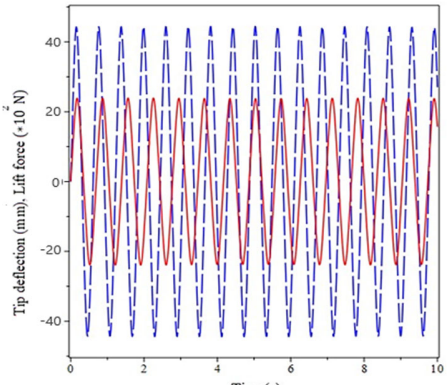

Fig. 9: Response of turbine end (blue broken line) and lift force (red continuous line) due to wind flow with a speed of 7.9 m/s

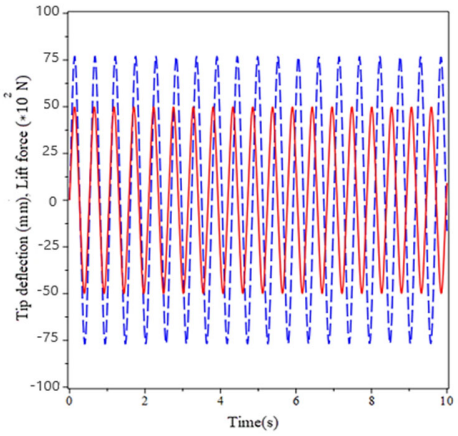

Fig. 10: Response of turbine end (blue broken line) and lift force (red continuous line) due to wind flow with a speed of 7.9 m/s

3. Numerical approach

In this section, by modeling the vortex bladeless turbine in ANSYS software as a 3D fluid-structure interaction, displacement of the vortex bladeless turbine, pressure, and velocity contours are obtained, and the results of the analytical section are validated. One of the most influential factors in the accuracy of turbulence modeling results is the Reynolds-Average Navier-Stokes (RANS) methods developed based on the averaging of Navier-Stokes equations. According to the advantages of the K-ω sst model, this model has been used in this project. The k-ω Shear Stress Transport (SST) turbulence model is widely used for simulating turbulent flows in computational fluid dynamics (CFD). It combines the advantages of the k-ω model (accurate near-wall treatment) and the k-ε model (robustness in free-stream regions). Here are the key advantages of the k-ω SST model.

- Accurate near-wall behavior
- Seamless transition between models
- Better prediction of separation that the vortex induced vibration is based on it.
- Suitable for a wide range of flows
- Reduced sensitivity to free-stream conditions

The following briefly describes the numerical solution and the vortex bladeless turbine model simulated using the ANSYS software. Table 2 shows the design parameters of the numerical solution.

Table 2: assumptions of Design parameters in 3D numerical solution

Velocity(m/s)	6.8
Mast Young's modulus (E) (GPa)	61.5
Rod Young's modulus (E) (GPa)	248.3
Mast length (cm)	100
Rod length(cm)	100
Mast diameter(mm)	100
Rod diameter(mm)	10
Mast thickness (mm)	2.5
Air density (kg/m3)	1.225
Displacement in the x direction	0
Displacement in the y direction	0
Inlet speed (m/s)	5.7-6.8-7.9
outlet relative pressure	0
Dynamic mesh model	on
Time conditions	Transient
Viscosity model	K-ω sst
Time step size	0.0005
Y+	1

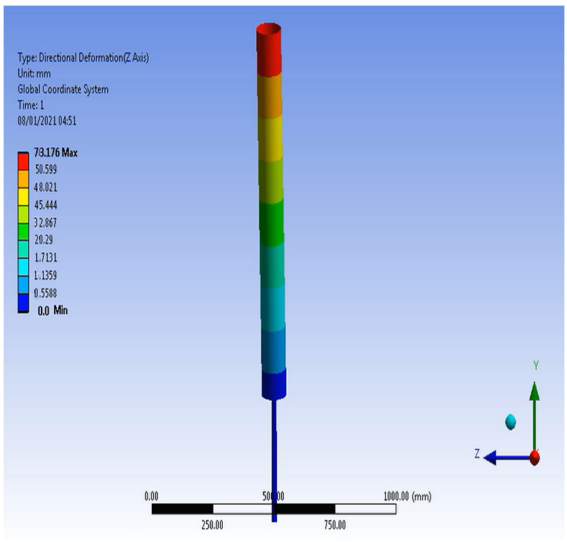

A high-quality mesh is one of the most important factors that must be considered to ensure the accuracy of the simulation. In solving the existing problem, the hybrid model and ICEM software are used to generate an organized mesh around the cylinder. A higher density is considered near the cylinder, while unstructured mesh with larger intervals is used farther away. This hybrid mesh is computationally less expensive and ensures the accuracy of the results in the critical region near the cylinder. Grid dependence is crucial in CFD problems since the simulation results will be unreliable if the grid is too large or small. A grid with a few elements yields inaccurate results, while a very large grid number leads to rounding errors, and the calculations may become computationally expensive. The maximum CG (Center of Gravity) deflection obtained at steady state for different numbers of grid elements is considered for the study of grid dependence, as shown in Figure 11. The number of grid elements increased until the maximum CG deflection did not change significantly. According to the results, the number of elements in the optimal grid structure in this research is 2110675, and the number of nodes is 4267731.

In the following, the velocity and pressure contours at different velocities and in the maximum state of changes are investigated, and the analytical solution results are evaluated.

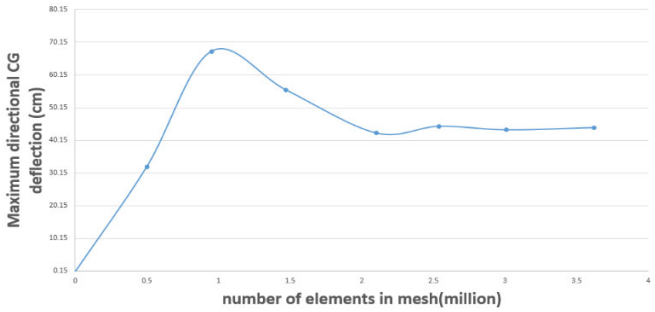

Fig11: Grid independency investigation

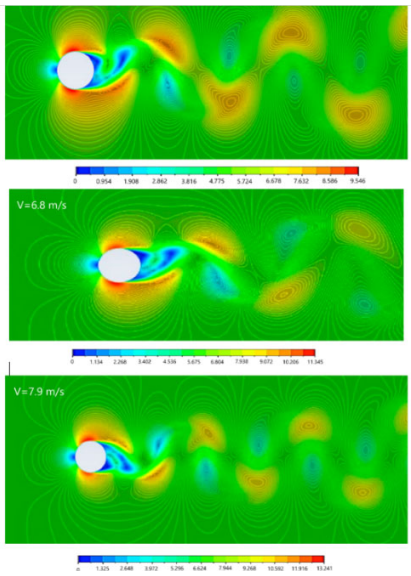

Fig. 12: Velocity contour in maximum mode with different flow speed

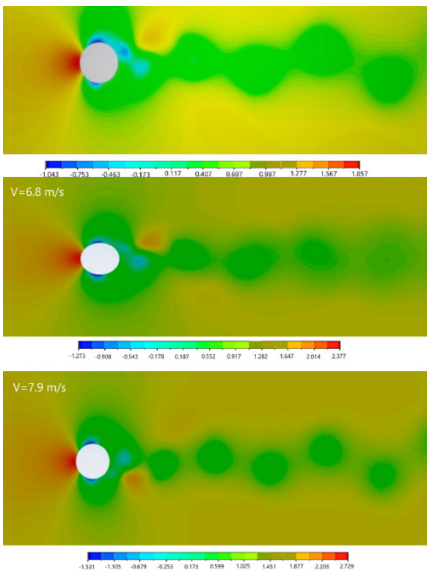

Fig. 13: Pressure contour in maximum mode with different flow speed

According to the velocity contours shown in Figure 12, the rate of velocity changes increases with the increase of fluid flow velocity. As seen in the pressure contour in Figure 13, the highest pressure occurs in the front part of the mast, which is the first point of contact of the fluid flow with the structure. It has a lower pressure around the mast, caused by the von Karman vortices, which is also the cause of the mast's vibration. The variation of lift force coefficient (C_L) and drag force coefficient (C_D) are investigated, and the results are shown in Figures 15 and 16, respectively. It can be seen that, with the increase in the frequency ratio, the drag force coefficient increases. However, the maximum lift force coefficient reaches its highest value close to a lock-in region.

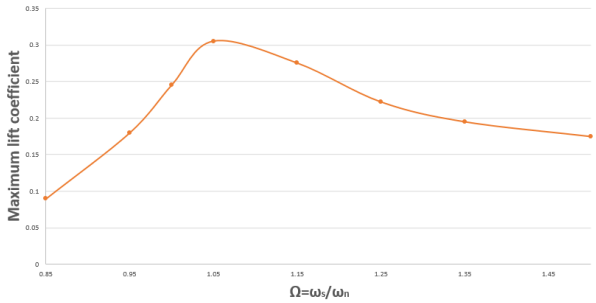

Fig. 15: The maximum Drag coefficient in the different frequencies

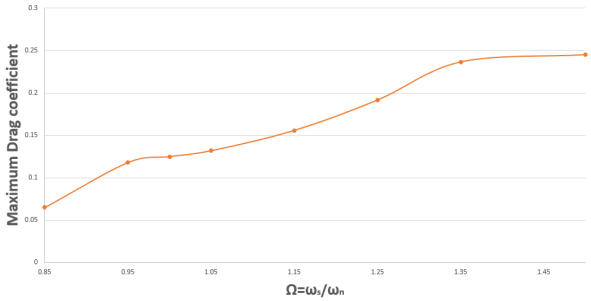

Fig. 16: The maximum Lift coefficient in the different frequencies

3.1. Verification of analytical relations with numerical solution

The displacement of the center of mass of the mast, that is, the connection point of the flexible base, is shown numerically and analytically in Figure 17. The investigation was carried out with a characteristic diameter of 100 mm and at different flow velocities. The analytical report is from equations 4 and 5, obtained using the 4th order of the Runge–Kutta numerical technique.

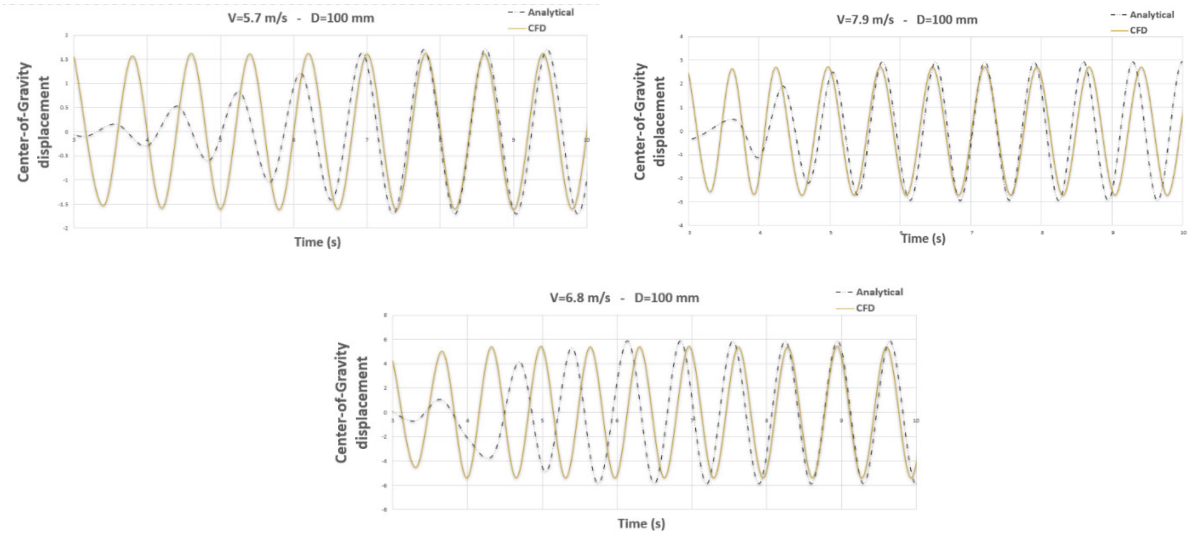

Fig. 17: Displacement of the center of mass of the mast with a characteristic diameter of 100 mm analytically and numerically at the speeds of 5.7, 6.8, and 7.9 m/s

On the other hand, the displacement ratio of the center of mass shows a difference of 5.5% at a speed of 5.7 m/s, about 8.2% at a speed of 6.8 m/s, and 8% at a speed of 7.9 m/s, which indicates the accuracy of the results. An acceptable solution is analytical relations. In the next part, the description and construction of the experimental sample of the turbine without vortex blades are discussed, and its performance is evaluated with the results obtained from the analytical relations.

4. Experimental test approach

In this section, the prototype of the vortex bladeless turbines is built, and the results will be evaluated with analytical results. In this regard, the vortex bladeless turbine is designed with the test structure using Solidworks software, as shown in Figure 18. This model is evaluated at different flow velocities. The displacement of the geometric center of the mast will be the basis for the validation of the prototype.

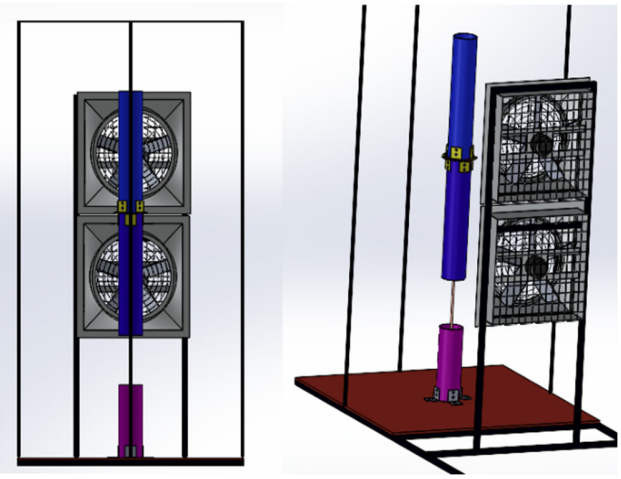

Fig. 18: Prototype design in Solidworks software

The laboratory sample in the current project consists of several parts, which will be briefly explained:

- **Mast and Elastic base**:

In the mast part, due to the required mechanical resistance and lightweight, GLASS RAIN FORCED PLASTIC (GRP) fiberglass cylinder is used (Table 3). A fibro carbon rod combines carbon fiber with adhesive, creating a strong, flexible, fatigue-resistant, and lightweight composite, making it a suitable choice for the base of a bladeless turbine (Table 3).

Table 3: Mast and base specification in experimental prototype

Mast Young's modulus (E) (GPa)	57.4
Mast length (cm)	100
Mast diameter(mm)	80-100-120
Mast thickness (mm)	2.5
Base Young's modulus (E) (GPa)	221
Base length (cm)	100
Base diameter(mm)	10

- **Flow simulator fan**

The flow we need in this project is a maximum of 8 meters per second; with the performed tests, an axial fan of 2800 revolutions with a capacity of 5500 cubic feet per minute was used, as shown in Figure 19a, which is adjusted with a single-phase dimmer, to reach the desired velocity.

- **Dimmer device, anemometer, and laser meter**

A dimmer is a device that can control the voltage in various electrical devices. The dimmer allows changing from the lowest voltage to the voltage of the power supply. In this research, the dimmer is used as a fluid flow speed controller by adjusting the input voltage to the fans. According to the fans' current consumption, a 5000 kVA dimmer is used. The anemometer device and laser meter were used to adjust the fluid flow and measure the displacement of the center of mass of the mast, respectively. These devices are depicted in Figures 19b and 19c, respectively.

Fig. 19: Simulator fan (a), anemometer (b) Laser distance meter (c)

Fig. 20: The experimental prototype

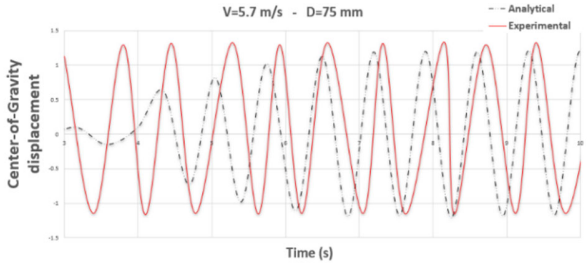

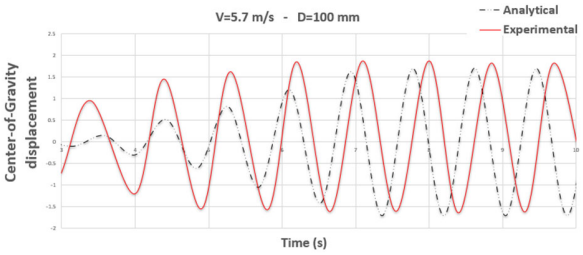

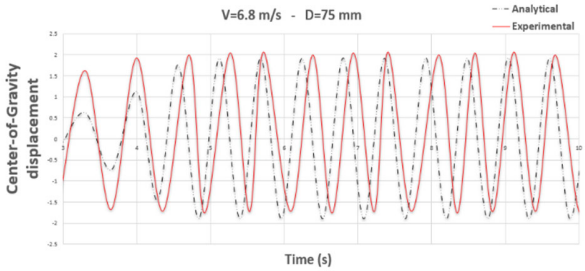

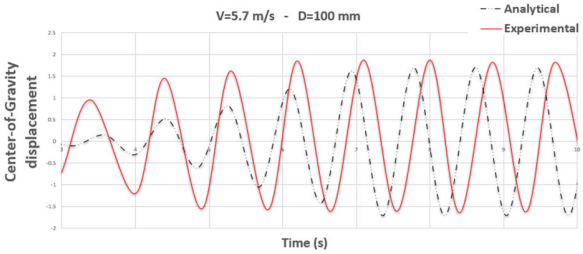

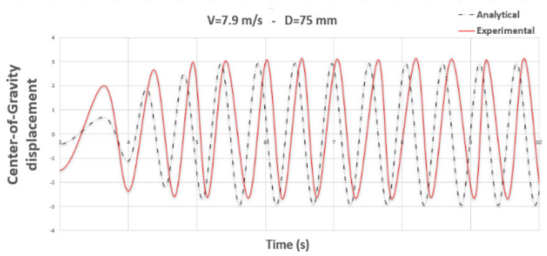

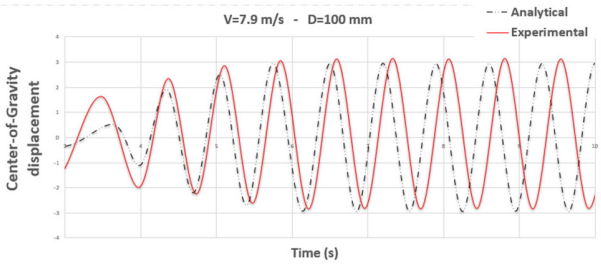

Fig. 21: Displacement of the center of mass of the mast with a characteristic diameter of 75 mm analytically and experimentally

Fig. 22: Displacement of the center of mass of the mast with a characteristic diameter of 100 mm analytically and experimentally

The experimental prototype is produced with the mentioned specifications and installed, as shown in Figure 20.

The bladeless turbine is designed in such a way that it is expected to be in the locked region at a speed of 6.8 m/s. The speed of the fluid was adjusted using a dimmer and anemometer. The vibration behavior of the system was investigated at different speeds, and the results are shown in Figures 21 to 23:

5. Conclusions

The main goal of this article is to present a method to optimize the vibration behavior of vortex bladeless turbines to increase energy harvesting, which is one of the emerging equipment for harvesting energy from airflow. To this end, the important parameters of the turbine, such as the characteristic diameter of the mast and flexible base, the height of the mast and flexible base, and other physical indicators, were locally optimized. The extracted nonlinear relationships were solved by the harmonic balance method, and the main physics parameters of the problem were extracted by considering the nonlinear factor and phenomena such as jump. The turbine was simulated in ANSYS software using the FSI method in the next part, and the pressure and velocity contours were presented at different frequencies. The results of the Euler-Bernoulli beam

analytical equations were evaluated with the results of the FSI coupling, which showed an average accuracy of 8%. The construction of a bladeless turbine is presented using the obtained design parameters and relevant references. The GRP was used to make the mast, and the fiberglass rod was used as a flexible rod. The most important key observations in this article are as follows:

1. Due to its efficiency, low construction cost, and easy installation, the vortex bladeless turbine can be used as an energy-harvesting device, which can complement a photovoltaic system, and it will perform well if it is properly locally optimized according to the relative conditions.
2. In analytical local optimization studies, the nonlinearity factor of the system is very important in the accuracy of the results. The jump phenomenon must be considered in the frequency analysis of various parameters.
3. Harvesting the energy of the vortex bladeless turbine in the areas close to the lock-in state, where the frequency coming from the fluid to the structure is near the structure's natural frequency, is desirable and produces multiple energy harvesting compared to other states.
4. The amount of energy harvested in the flow direction is very small and can be considered zero in calculations, which helps increase the speed of calculations and reduce costs.
5. The accuracy of the analytical solution will be better estimated in the ratio of frequencies further away from the lock-in frequency.
6. The ratio of lift force to displacement increases with the increase of the Reynolds number, which indicates better turbine performance at higher speeds.
7. The frequency ratio of analytical relations, compared to the numerical solution, is 5.2% at the speed of 5.7 m/s, 6.4% at the speed of 6.8 m/s, and 6.0% at the speed of 7.9 m/s, which is generally acceptable. On the other hand, the displacement ratio of the center of mass shows a difference of 5.5% at the speed of 5.7 m/s, about 8.2% at the speed of 6.8 m/s, and 8% at the speed of 7.9 m/s, Considering the simplifying assumptions in the analytical relationships and the complexity of the phenomenon of induced vibrations, the accuracy of the solution is acceptable.

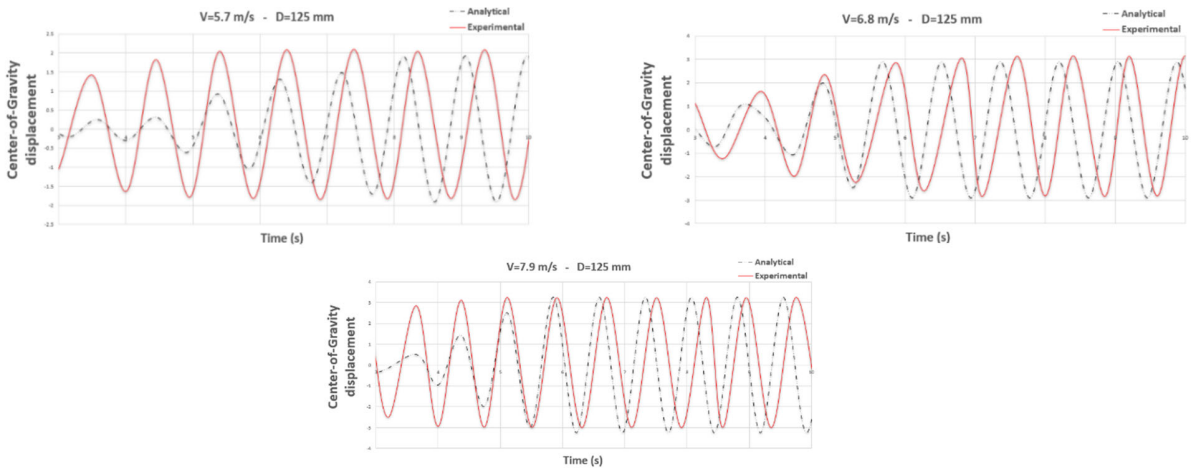

Fig. 23: Displacement of the center of mass of the mast with a characteristic diameter of 125 mm analytically and experimentally

The frequency of the analytical equations compared to the average frequency of the experimental test is 6% at the velocity of 5.7 m/s, 10.5% at the velocity of 6.8 m/s, and 8% at the velocity of 7.9 m/s. There are differences, which is generally acceptable considering the non-ideality of the test conditions. On the other hand, the displacement ratio of the center of mass shows a difference of 6.5% at a velocity of 5.7 m/s, about 11% at a velocity of 6.8 m/s and 9% at a velocity of 7.9 m/s. Better results can be achieved by using a DC fan and a diffuser to direct the fluid flow.

References

[1] Renewable Energy and Energy Efficiency Organization in Iran, in.

[2] International Renewable Energy Agency (IRENA), in.

[3] E. Dobrucali, O.K. Kinaci, URANS-based prediction of vortex induced vibrations of circular cylinders, Journal of Applied Fluid Mechanics, 10 (2017) 13.

[4] S.M. Hosseinalipoor, H. Haji ghafoori boukani, Numerical investigation of flow past a circular cylinder beneath a free surface with volume of fluid method, Amirkabir J. Mech. Eng, 49 (2017) 8.

[5] A. Chizfahm, E. Azadi Yazdim, M. Eghtesad, Dynamic modeling of vortex induced vibration wind turbines, Renewable Energy, 121 (2018) 12.

[6] J.S. Cajas, G. Houzeaux, D.J. Yáñez, M. Mier-Torrecilla, Shape project vortex bladeless: parallel multi-code coupling for fluid-structure interaction in wind energy generation, in, Barcelona Supercomputing Center, Centro Nacional de Supercomputación, 2016.

[7] I. Bahadur, Dynamic modeling and investigation of a tunable vortex bladeless wind turbine, Energies, 15 (2022) 6773.

[8] M.S. Raghuwanshi, A. Sonanis, A. Pandey, A. Shrivastava, M. Banwariya, C.S. Mourya, Design and fabrication of vortex bladeless turbine, in, SSRN Electronic Journal, 2021.

[9] S. Saengsaen, C. Chantharasenawong, T. Liang Wu, A 2–D mathematical model of vortex induced vibration driven bladeless wind turbine, in: The 3rd International Conference on Mechanical, System and Control Engineering (ICMSC 2019), EDP Sciences, MATEC Web of Conferences 291, 02007, 2019.

[10] O.D. Kshirsagar, A.B. Gaikwad, Design and analysis of vortex bladeless windmill for composite material Journal of Industrial Mechanics 4(2023) 15-24.

[11] S. Bagheri, E. Farahani, M. Mohammadpour, H. Zandi, P. Safarpour, M. Zandi, Investigation of nonlinear energy harvesting from vortex induced vibrations in vortex bladeless turbines, in: 7th Iran Wind Energy Conference (IWEC 2021), Shahrood University of Technology, Shahroud, Iran., 2021.

[12] J. Jauvtis, C. Williamson, Vortex-induced vibration of a cylinder with two degrees of freedom, Journal of Fluids and Structures, 17 (2003) 1035-1042.

[13] J. Carberry, R. Govardhan, J. Sheridan, D. Rockwell, C. Williamson, Wake states and response branches of forced and freely oscillating cylinders, European Journal of Mechanics B-fluids, 23 (2002) 89-97.

[14] T. Sarpkaya, A critical review of the intrinsic nature of vortex-induced vibrations, Journal of Fluids and Structures, 19 (2004) 389-447.

[15] E. Bush, L. Manuel, Foundation models for offshore wind turbines, in: 47th AIAA Aerospace Sciences Meeting including The New Horizons Forum and Aerospace Exposition, AIAA, 5-8 January, Orlando, Florida, USA., 2009.

[16] J. Jianhong Wang, D. Qin, T.C. Lim, Dynamic analysis of horizontal axis wind turbine by thin-walled beam theory, Journal of Sound and Vibration, 329 (2010) 3565-3586.

[17] J. Jie Chen, D. Jiang, Modal analysis of wind turbine tower, in: World Non-Grid-Connected Wind Power and Energy Conference, IEEE, 5-7 November, Nanjing, China, 2010.